

Microstructure development and piezoelectric properties of highly textured CuO-doped KNN by templated grain growth

Yunfei Chang

Department of Materials Science and Engineering, and Materials Research Institute, Pennsylvania State University, University Park, Pennsylvania 16802; and School of Chemistry and Materials Science, Shaanxi Normal University, Xi'an, 710062 Shaanxi, People's Republic of China

Stephen F. Poterala

Department of Materials Science and Engineering, and Materials Research Institute, Pennsylvania State University, University Park, Pennsylvania 16802

Zupei Yang

School of Chemistry and Materials Science, Shaanxi Normal University, Xi'an, 710062 Shaanxi, People's Republic of China

Susan Trolier-McKinstry and Gary L. Messing^{a)}

Department of Materials Science and Engineering, and Materials Research Institute, Pennsylvania State University, University Park, Pennsylvania 16802

(Received 18 October 2009; accepted 22 December 2009)

This paper demonstrates the production of $\langle 001 \rangle$ -oriented CuO-doped ($K_{0.476}Na_{0.524}$) NbO_3 (KNN) piezoelectric ceramics with a polymorphic phase transition (PPT) temperature greater than 180 °C by templated grain growth (TGG) using high aspect ratio $NaNbO_3$ template particles. A novel (to the KNN system) two-step sintering and annealing process combined with CuO doping is demonstrated to improve density and maximize texture quality ($F_{001} = 99\%$ and rocking curve FWHM = 6.9°) in textured KNN ceramics. The best electromechanical properties ($k_p \approx 0.58$, $k_{31} \approx 0.33$, $d_{33} \approx 146$ pC/N, $T_{o-t} \approx 183$ °C, $T_c \approx 415$ °C, $\epsilon_r = 202$, and $\tan \delta = 0.016$) are achieved in 1 mol% CuO-doped KNN with $F_{001} = 99\%$ and a relative density of 96.3%. The values of d_{33} , k_p , and k_{31} are 70–90% higher than randomly oriented ceramics and are obtained without a significant reduction in the PPT temperature, resulting in stable piezoelectric performance over a wide temperature range (–50 to 180 °C). These results show that high-quality textured KNN can be obtained by TGG and that a reactive matrix is unnecessary.

I. INTRODUCTION

Lead-based perovskites like $Pb(Zr_xTi_{1-x})O_3$ (PZT) ceramics dominate the commercial piezoelectric market for sensors, actuators, and transducers, because they have excellent dielectric and piezoelectric properties near the morphotropic phase boundary (MPB) and can operate from –50 to 150 °C.¹ However, the toxicity of lead has raised environmental and health concerns and prompted extensive research worldwide to develop lead-free piezoelectric materials.²

Pure (K,Na) NbO_3 has a rhombohedral-orthorhombic phase transition temperature of about –160 °C, an ortho-

rhombic-tetragonal polymorphic phase transition (PPT) temperature of ~200 °C and a Curie temperature of ~400 °C, resulting in a wide operating temperature range.^{1–3} However, pure (K,Na) NbO_3 is difficult to sinter to high density and has relatively low room-temperature electromechanical properties.^{3,4} Modified (K,Na) NbO_3 systems can partially overcome these problems and have attracted attention following the report of textured (K,Na,Li)(Nb,Ta,Sb) O_3 ceramics with a piezoelectric coefficient d_{33} of up to 416 pC/N.⁵ Subsequently, many researchers have explored the effects of Li-, Ta-, and/or Sb-ionic substitutions on the electromechanical properties of randomly oriented (K,Na) NbO_3 ceramics.^{6–11} These studies show vast increases in the room-temperature dielectric constant and piezoelectric coefficients with A- and/or B-site substitutions, but these improvements were achieved by shifting the PPT to near room temperature. Consequently, the low-field room-temperature electromechanical properties are strongly temperature dependent and the material is of limited use for most

^{a)}Address all correspondence to this author.

e-mail: messing@ems.psu.edu

This author was an editor of this journal during the review and decision stage. For the *JMR* policy on review and publication of manuscripts authored by editors, please refer to http://www.mrs.org/jmr_policy

DOI: 10.1557/JMR.2010.0084

applications. The associated high-field properties show comparatively small temperature dependence,⁵ but this effect is related to additional strain hysteresis at high temperatures. Some sintering aids, such as CuO, ZnO, and $K_4CuNb_8O_{23}$,^{12–16} improve the sinterability of (K,Na)NbO₃ ceramics without significantly shifting the PPT temperature, but result in only minor enhancement in piezoelectric response ($k_p \leq 0.45$, and $d_{33} \leq 120$ pC/N) because of improved density and microstructure.

Crystallographic texturing of polycrystalline ferroelectric ceramics, such as $Pb(Mg_{1/3}Nb_{2/3})O_3$ – $PbTiO_3$ (PMN–PT),^{17–19} $Pb(Mg_{1/3}Nb_{2/3})O_3$ – $Pb(Zr,Ti)O_3$ (PMN–PZT),¹⁹ $Bi_{0.5}(Na,K)_{0.5}TiO_3$,^{20,21} $Sr_{0.53}Ba_{0.47}Nb_2O_6$,²² and $(K,Na,Li)(Nb,Ta,Sb)O_3$,⁵ results in greatly enhanced piezoelectric properties that can reach $\geq 50\%$ of single-crystal values.²³ Crystallographic texture is most effectively produced using the templated grain growth (TGG) method. In TGG, texture is developed by sintering and annealing compacts containing large (typically 5–50 μm) template particles and fine matrix powder of the target ceramic composition and phase. Epitaxial growth of the matrix composition on the aligned template particles is driven by the difference in the surface free energy between the matrix grains and the larger template particles. If a reactive matrix is used, the template particles may also serve as heterogeneous nucleation sites for formation of the desired phase. This process is referred to as reactive TGG (RTGG).

Excellent room-temperature properties in $(K,Na,Li)(Nb,Ta,Sb)O_3$ were obtained by Saito et al.⁵ by shifting the PPT to near room temperature and by texturing by the RTGG method (KNbO₃ matrix, NaNbO₃ matrix, and NaNbO₃ template as starting materials). In a later paper, the same group textured CuO-doped $(K_{0.5}Na_{0.5})NbO_3$ by RTGG and investigated the microstructural evolution and texture development in this system.²⁴ The authors report d_{33} and k_p values of 123 pC/N and 0.54, respectively, about 43% higher than those of randomly oriented ceramics. However, TGG or RTGG studies in other perovskite systems suggest that better performance can be obtained in $(K,Na)NbO_3$ based ceramics. For example, $\geq 70\%$ and $\geq 60\%$ improvements in response are seen in PMN–PT and $Na_{1/2}Bi_{1/2}TiO_3$ – $BaTiO_3$ systems, respectively.²³ These enhancements are directly related to the anisotropy of piezoelectric response in the single-crystal state. Because there are few reports on the electromechanical properties of KNN crystals, additional work is needed to determine if the observed lower performance enhancement in textured KNN ceramics is an artifact of processing conditions. Additionally, most work on textured $(K,Na)NbO_3$ to date has focused on RTGG processing using a mixed NaNbO₃ and KNbO₃ matrix. This additional complexity may not be necessary or helpful, as the principal benefit of RTGG (nucleation of the target structure on the template surfaces) is defeated by the use of perovskite phases in the matrix composition. Also, standard TGG

processing yields very high texture quality in $(K_{0.5}Na_{0.5})(Nb_{0.97}Sb_{0.03})O_3$ ceramics.²⁵

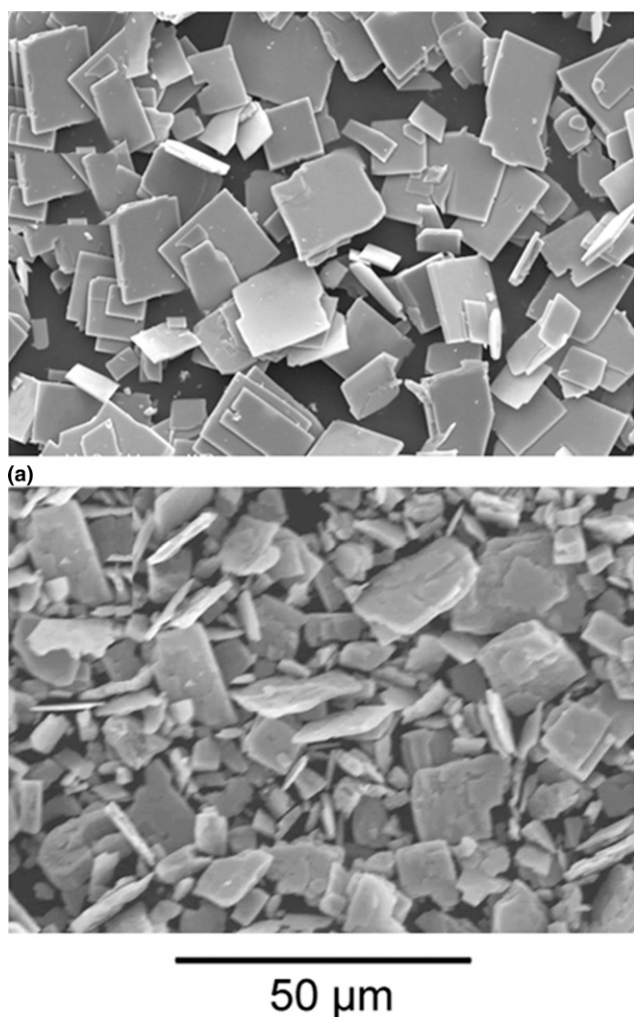
In this paper, the MPB composition $(K_{0.476}Na_{0.524})NbO_3$ (KNN),^{1,3} which has a PPT temperature of ~ 200 °C, was textured using NaNbO₃ template particles (denoted NN_T) by the TGG process. These templates can be readily synthesized by topochemical microcrystal conversion (TMC)²⁶ and are compositionally compatible with KNN.^{5,24,25} During TMC, the templates inherit the high aspect ratio of a layered precursor phase ($Bi_{2.5}Na_{3.5}Nb_5O_{18}$) during a topochemical (topotactic or epitaxial) chemical conversion reaction.^{5,24} The templates are fully isostructural with KNN at high temperature and are ideal substrates for TGG. Also, the eventual solid solution between the templates and KNN matrix may not result in loss of ceramic performance or temperature stability due to chemical modification of the host ceramic. Eventual homogenization of the final ceramic avoids electric field dilution or mechanical clamping of the textured grains that can be caused by residual template particles.^{17,19,23} CuO was used as a liquid-phase sintering aid to alleviate stresses from constrained sintering around the template particles. The effects of CuO doping on densification, microstructure evolution, and template growth during sintering process are discussed. Preliminary dielectric and piezoelectric properties of the textured ceramics produced by TGG are reported and correlated with CuO content (which acts as an acceptor dopant in KNN). The temperature dependence of piezoelectric response for textured CuO-doped KNN is also presented in this work.

II. EXPERIMENTAL PROCEDURE

A. Sample preparation

Platelike NaNbO₃ template particles (NN_T) were prepared by the topochemical microcrystal conversion (TMC) process.²⁶ $Bi_{2.5}Na_{3.5}Nb_5O_{18}$ template precursor particles of 1 to 2 μm in thickness by about 10 to 20 μm in length were synthesized from a mixture of Bi₂O₃ (Alfa Aesar, Ward Hill, MA, 99%), Na₂CO₃ (EMD Chemicals Inc., Gibbstown, NJ, 99.5%), and Nb₂O₅ (Strem Chemicals, Newburyport, MA, 99.5%) at 1125 °C for 2 h using molten NaCl (Mallinckrodt Chemicals, Phillipsburg, NJ, 99%) [Fig. 1(a)]. NaNbO₃ template particles were synthesized in molten NaCl from a mixture of $Bi_{2.5}Na_{3.5}Nb_5O_{18}$ and Na₂CO₃ for 6 h at 975 °C. The tabular NaNbO₃ template particles were about 0.5 to 2 μm in thickness by about 10 to 20 μm in length [Fig. 1(b)].

Equiaxed powders of 0.4–0.5 μm of $(K_{0.5}Na_{0.5})NbO_3$ - x mol% CuO were prepared by the conventional mixed oxide (CMO) process. Na₂CO₃ (EMD Chemicals Inc., 99.5%), Nb₂O₅ (H.C. Starck, Newton, MA, 99.9%), K₂CO₃ (Alfa Aesar, Heysham Lancs, UK, 99%), and CuO (Sigma-Aldrich, St. Louis, MO, 99.99%) were milled in ethanol for 3 days and calcined at 800 °C for



(a)
(b)
FIG. 1. Scanning electron micrographs of (a) Bi_{2.5}Na_{3.5}Nb₅O₁₈ template precursor particles and (b) NaNbO₃ template particles synthesized by the topochemical microcrystal conversion process.

6 h. For the TGG process, 1 mol [(K_{0.5}Na_{0.5})NbO₃ – *x* mol% CuO (*x* = 0, 0.5, and 1.0)] matrix powder and 0.05 mol NN_T were mixed to obtain a CuO-doped (K_{0.476}Na_{0.524})NbO₃ final composition. Tape casting slurries were mixed by dispersing the powders (23.56 vol%) in a xylene-ethanol solution (64.02 vol%) containing blown menhaden fish oil (2.14 vol%), polyvinyl butyral, (5.35 vol%), butyl benzyl phthalate, (2.39 vol%), and polyalkylene glycol, (2.54 vol%). The pseudoplastic slurries were tape cast at a rate of 37.5 cm/min. The dried tapes with about 70 μm in thickness were cut, stacked, and laminated at 75 °C and 20 MPa for 1 h to fabricate 1.3 and 5 mm thick green compacts before sintering. Organics were removed by heating to 600 °C for 6 h in air. The green parts were isostatically pressed at 200 MPa for 3 min before sintering in O₂ to 1115 °C for 4 h to promote densification. The samples were then annealed between 1115 and 1160 °C for 1–12 h (depending on CuO concen-

tration) to promote template growth. The ideal annealing conditions for each composition are discussed later. For comparison, randomly oriented ceramics of CuO-doped (K_{0.476}Na_{0.524})NbO₃ were fabricated by the CMO method. Textured samples were removed from the furnace at temperatures between 700 and 1115 °C to characterize the phase structure and microstructure evolution during the sintering step.

B. Characterization

The phase structure and the degree of texture were determined by x-ray diffraction (XRD) with Cu Kα radiation (PAD V, Scintag, Inc., Cupertino, CA) on sample surfaces cut parallel to the tape casting plane. The degree of pseudo-cubic ⟨001⟩ orientation of the textured ceramics was estimated using the Lotgering factor F_{001} , and was calculated from the relative peak intensities between 20 and 60° 2θ for random-oriented and textured KNN.²⁷ Although the Lotgering factor is convenient to calculate, it does not fully characterize texture quality because slightly misoriented grains are not detected. Therefore, rocking curve data around the 002 peak was collected to determine the width (full width at half maximum, or FWHM) of the grain orientation distribution. The data were corrected using the NIST TexturePlus software program (M.D. Vaudin, National Institute of Standards and Technology, Ceramics Division, Gaithersburg, MD) to eliminate background, defocus, and absorption effects.¹⁷

The shrinkage of 5 mm thick green samples was measured using thermomechanical analysis (TMA-50, Shimadzu Corp., Kyoto, Japan) with the same heating profile as used for sintering. The densities of the sintered samples were measured by Archimedes' method, and the theoretical densities of sintered samples were calculated using lattice parameters obtained by XRD measurements. Fracture surfaces and thermally etched cross sections of various orientations were imaged using scanning electron microscopy (SEM; FEI Quanta 200, Hillsboro, OR) to observe final and intermediate microstructures.

Ceramic disks 0.5 mm thick and 10 mm in diameter and plates measuring 10 × 3 × 0.6 mm (with the pseudocubic ⟨001⟩ in the thickness direction) were cut from fully annealed specimens to measure the planar and extensional electromechanical-coupling factors k_p and k_{31} , respectively. Samples were electroded with fire-on-silver paste (DuPont 6160, DuPont Microcircuit Material, Research Triangle Park, NC) on the upper and lower surfaces and were poled for 10 min at 120 °C with an applied field of 3 kV/mm. The dielectric constant (ϵ_r) and dielectric loss ($\tan \delta$) were measured as a function of temperature at 1 kHz using an LCR meter (HP4284) on heating in a furnace. The piezoelectric constant d_{33} was measured from 1-day aged samples using a Berlincourt d_{33} meter (ZJ-2, Institute of Acoustics Academia Sinica, Beijing, China).

The electromechanical-coupling factors k_p and k_{31} were determined by the resonance and antiresonance techniques with an impedance analyzer (HP4294A) in accordance with the IEEE standards on piezoelectricity.^{28,29}

III. RESULTS AND DISCUSSION

The relative density and *z*-direction ($\langle\langle 001 \rangle\rangle$) shrinkage of templated samples were plotted as a function of temperature and CuO concentration during the sintering step (shown in Fig. 2). All samples shrink at nearly the same rate up to 850 °C (and reach nominally 62% density) regardless of CuO content. Above 850 °C, the CuO-doped samples shrink more rapidly than the undoped samples. The 0.5% and 1% CuO-doped samples have similar shrinkage ($\sim 12.8\%$) up to 980 °C (compared with 6.0% shrinkage for the pure KNN). Above 980 °C, the 1% CuO-doped samples shrink slightly faster than the 0.5% CuO samples. The 0.5% and 1% CuO-doped KNN samples reach final densities of 90.2% and 91.8% at 1115 °C (no hold), respectively, while undoped KNN reaches a density of 86.6%. Densities near or exceeding 92% are required for template growth because of the inhibiting effects of porosity on grain-boundary mobility.²³ The rapid increase in shrinkage rate above 850 °C in CuO-doped samples suggests that the samples sinter by a liquid phase mechanism (caused by a reaction between CuO and the KNN matrix powder). The eutectic point (~ 1020 °C)³⁰ between

Nb_2O_5 and CuO indicates that a liquid phase should be present at higher temperature, but the composition of the liquid phase below 1000 °C was not elucidated because the Na_2O –CuO and K_2O –CuO phase diagrams do not exist in the literature. As proposed by Matsubara et al.,¹⁵ it is possible that a liquid phase with a composition near $\text{K}_4\text{CuNb}_8\text{O}_{23}$ forms around 1050 °C.

Figure 3 shows scanning electron micrographs of the fracture surfaces of 1% CuO-doped KNN samples removed on sintering at 1000 °C (no hold), 1100 °C (no hold), and 1115 °C (4 h). The templates show a uniform distribution and are surrounded by 0.5 μm matrix grains during sintering up to 1100 °C. Strong bonding of the templates and matrix grains occurs after 1100 °C, evidenced by the change in fracture behavior of the templates from intergranular in Figs. 3(a) and 3(b) to transgranular in Figs. 3(c) and inset 3(d). As observed in Fig. 3(d), templated KNN doped with 1 mol% CuO shows moderate density after sintering for 4 h at 1115 °C without substantial template growth.

Figure 4 shows the phase evolution of 1% CuO-doped, templated KNN samples during the sintering process from 1000 to 1115 °C. After 4 h at 1115 °C, the intensity of the NN_T template peaks begins to decrease as a result of the reaction of the template particles with the matrix. As shown later, the templates react and form a solid solution with the KNN matrix during the higher-temperature growth anneal. No significant texture development

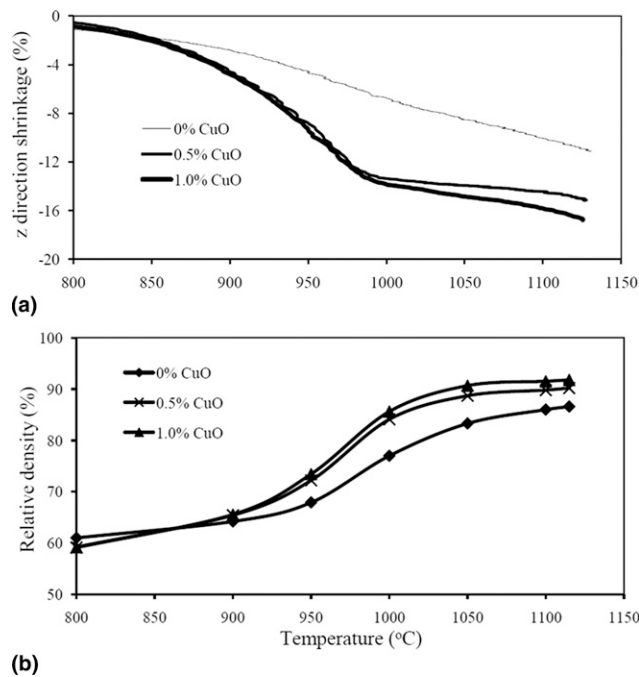


FIG. 2. The (a) linear shrinkage in the *z*-direction (perpendicular to the tape casting plane) and (b) densification behavior of the KNN samples doped with 0, 0.5, and 1% CuO and produced by TGG (heated at 4 °C/min).

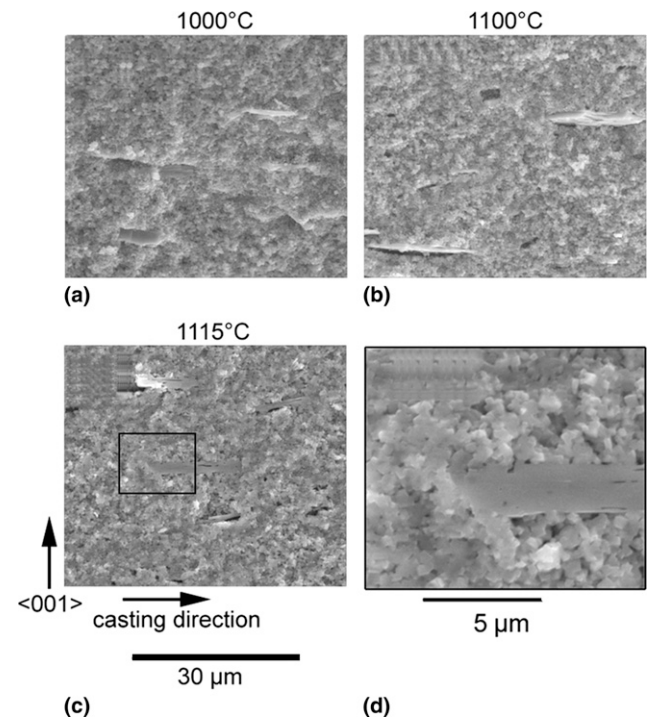


FIG. 3. Scanning electron micrographs of the fracture surface of the samples doped with 1% CuO and produced by TGG at (a) 1000 °C (no hold time), (b) 1100 °C (no hold time), and (c, inset d) 1115 °C for 4 h.

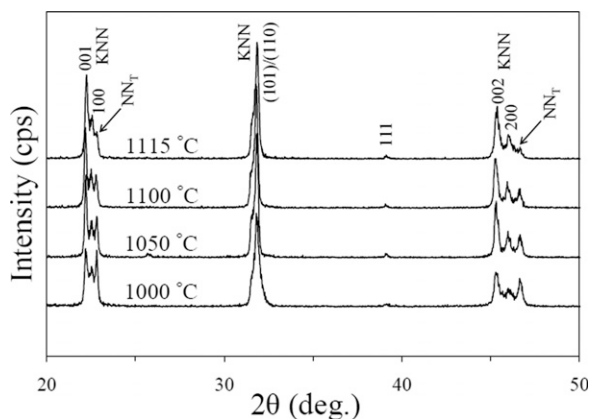


FIG. 4. XRD patterns of the samples doped with 1.0% CuO and produced by TGG heated at 1000 °C (no hold time), 1050 °C (no hold time), 1100 °C (no hold time), and 1115 °C for 4 h. The XRD profile is indexed using pseudo-tetragonal Miller indices. NN_T refers to the $NaNbO_3$ template phase.

occurs in these samples during the sintering step, as evidenced by the low intensity of the 001, 100, 002, and 200 pseudo-tetragonal peaks compared with the 101/110 100% intensity peak.

Annealing of the densified KNN samples to complete final-stage densification and promote template growth was done at just under the solidus temperature of the KNN matrix composition (about 1160 °C for pure KNN). Care is required to anneal at these temperatures as the solidus temperature is reduced by CuO doping. Through a series of carefully controlled experiments, the ideal annealing conditions for texture development were determined as a function of CuO content. Maximum texture development was observed in pure KNN at 1150 °C, but occurred at lower temperatures for CuO-doped KNN (1135 °C for 0.5% CuO and 1125 °C for 1% CuO). Additionally, the annealing time required to reach full texture was reduced by CuO doping (from 8 h for pure KNN to 3 h for 0.5 and 1% CuO). The final density of textured KNN samples also increased as a function of CuO content, from 92.1% for pure KNN to 95.4% and 96.3% for 0.5% and 1% CuO-doped KNN, respectively.

The calculated Lotgering factor F_{001} of the $\langle 001 \rangle$ orientation is plotted as a function of relative density in Fig. 5, for both optimum and suboptimum annealing conditions. The annealing conditions for each sample (in addition to the densification step) are indicated in the figure. The limiting effect of pore drag on boundary mobility produces a distinct relationship between final density and texture fraction. The data points for pure and CuO-doped KNN fall on the same trend, showing that the final texture quality is not controlled directly by liquid phase content but indirectly by the sample density. This result is in contrast to those seen in textured PMN-PT ceramics, where a PbO liquid phase is required to attain high texture quality in dense samples. The highest

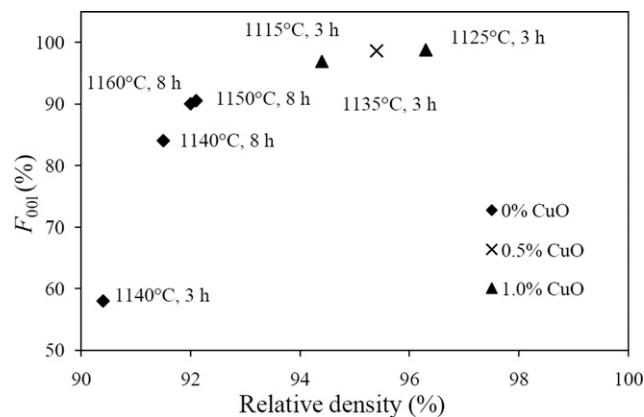


FIG. 5. Lotgering factors of $\langle 001 \rangle$ textured KNN ceramics doped with 0, 0.5, and 1.0% CuO as a function of relative density. All samples were sintered at 1115 °C for 4 h before annealing at the indicated conditions.

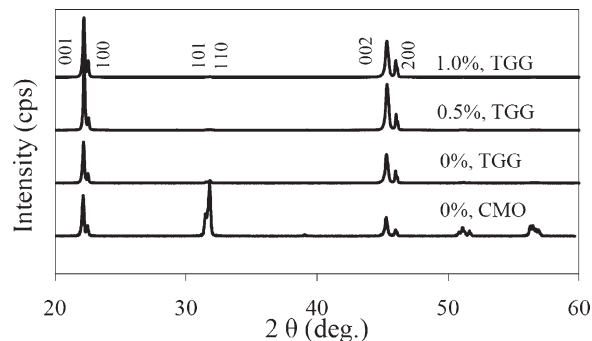


FIG. 6. XRD patterns of the textured ceramics doped with 0, 0.5, and 1.0% CuO sintered at 1150 °C for 8 h, 1135 °C for 3 h, and 1125 °C for 3 h, respectively. The XRD profiles are indexed using pseudo-tetragonal Miller indices.

density and texture fraction was obtained in 1% CuO-doped KNN annealed at 1125 °C for 3 h (after sintering at 1115 °C for 4 h as described previously). The same composition annealed at 1115 °C for 3 h (a combined sintering and annealing run at 1115 °C for 7 h) reached a lower final density and texture quality. At all CuO doping levels, the best densities and texture fractions were obtained using a two-step thermal processing route with a sintering step at 1115 °C. Sintering temperatures greater than 1115 °C resulted in no template growth, as the templates were damaged by excessive reaction with the KNN matrix.

The XRD patterns of randomly oriented and textured KNN ceramics, sintered for 1115 °C for 4 h and annealed at the ideal conditions described above, are shown in Fig. 6. All of the ceramics are phase pure perovskite and have the orthorhombic structure. The Lotgering factors (F_{001}) of the pure KNN reached a maximum of 90%, while the 0.5 and 1.0% CuO-doped KNN both reach 99%. As expected, texturing with $NaNbO_3$ templates

does not shift the KNN peak positions, but the addition of 0.5 mol% CuO causes a shift to higher 2θ values, reflecting the presence of oxygen vacancies induced by substitution of Cu^{2+} for Nb^{5+} on the B site of KNN. Increasing the CuO doping level to 1% does not further shift the KNN peak positions, suggesting the solubility limit of Cu^{2+} in the KNN lattice is ≤ 0.5 mol% CuO.

Rocking curves of the textured ceramics around the 002 peak are compared in Fig. 7. Undoped KNN ceramics have low peak intensity and a full width at half-maximum (FWHM) of 12.6° . The rocking curve peak intensity is much higher for the CuO-doped samples, and the FWHM decreases to 8.5° for 0.5% CuO-doped KNN and to 6.9° for 1% CuO-doped KNN. Because the template alignment is determined by the tape casting step and not during thermal processing, the increase of FWHM at lower CuO contents is an artifact of the lower texture volume fraction. These FWHM values are comparable to those obtained in PMN-PT textured ceramics ($\sim 7^\circ$) that show a $\geq 70\%$ increase in piezoelectric response compared with random ceramics.

Scanning electron micrographs of polished and thermally etched textured KNN ceramics are shown in Fig. 8. The undoped textured ceramic has a relatively heterogeneous microstructure composed of small matrix grains, large textured grains, and voids [Fig. 8(a)]. (Even after annealing at 1160°C for 8 h, the relatively low density of this sample results in a relatively low orientation degree). Doping with 0.5% or 1.0% CuO results in a more uniform, coarse-grained microstructure [Figs. 8(b) and 8(c)]. According to EDS analysis, K, Na, and Nb are evenly distributed throughout the textured ceramics. Based on the data presented in Figs. 5–8, it can be seen that CuO is an effective sintering aid and leads to high density (and therefore high texture quality) in KNN ceramics fabricated by TGG.

Table I shows the dielectric and piezoelectric properties of randomly oriented and textured KNN ceramics as

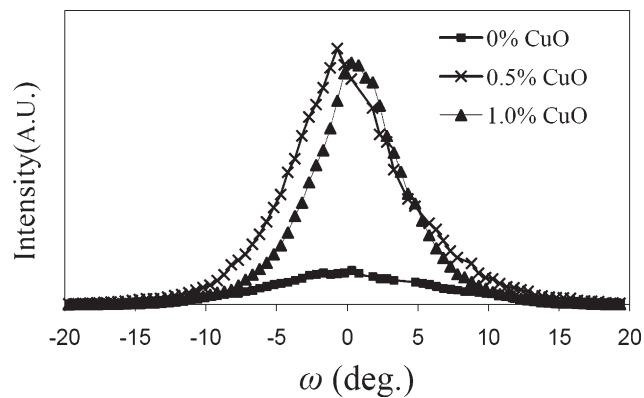


FIG. 7. Rocking curves around the 002 peak of the $\langle 001 \rangle$ textured KNN ceramics doped with 0, 0.5, and 1.0% CuO sintered at 1150°C for 8 h, 1135°C for 3 h, and 1125°C for 3 h, respectively.

a function of CuO content. The textured pure KNN has a PPT temperature (T_{o-t}) of 209°C , and a Curie temperature T_c of 420°C ; these values are nearly the same as those of randomly oriented KNN ceramics. Doping with 1% CuO slightly reduces T_{o-t} and T_c to 183 and 415°C , respectively. A comparable drop is observed in 1% CuO-doped randomly oriented KNN. The decrease in T_{o-t} and T_c relative to pure KNN may be caused by a slight Cu^{2+} -induced lattice distortion of KNN. However, the PPT temperature of CuO-doped KNN remains high and should lead to good stability of material properties over a wide temperature range. The d_{33} , k_p , and k_{31} of textured pure KNN are 135 pC/N, 0.45 , and 0.29 , respectively (20–50% better than those of randomly oriented pure KNN). In comparison, the d_{33} , k_p , and k_{31} values of textured 1% CuO–KNN are improved to 146 pC/N, 0.58 , and 0.33 , respectively, from the random ceramic values of 85 pC/N, 0.31 , and 0.17 (representing a 70–90% improvement). The ϵ_r and $\tan \delta$ of KNN ceramics at all CuO contents were relatively unchanged by texturing.

The values of piezoelectric constant d_{33} obtained in this study are strongly dependent on the presence of

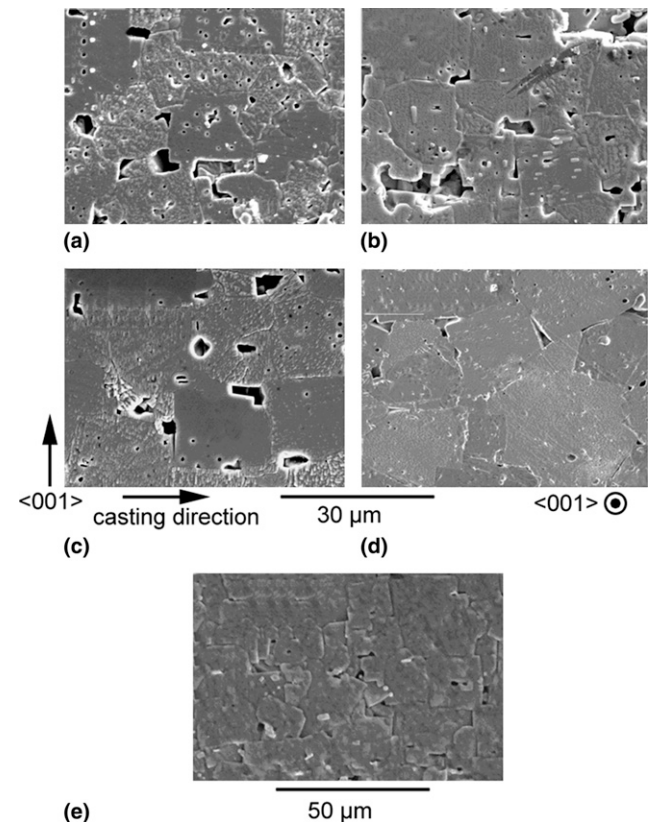


FIG. 8. Scanning electron micrographs of textured KNN doped with (a) 0% CuO, (b) 0.5% CuO, and (c) 1.0% CuO (cut parallel to $\langle 001 \rangle$ and thermally etched) sintered at 1150°C for 8 h, 1135°C for 3 h, and 1125°C for 3 h, respectively. (d) and (e) show an etched longitudinal section (cut perpendicular to $\langle 001 \rangle$) and as-fired cross section of textured KNN–1% CuO.

TABLE I. Dielectric and piezoelectric properties of the randomly oriented and textured ceramics as a function of CuO doping.

CuO composition (mol%)	$x = 0$ random	$x = 0$ textured	$x = 0.5$ random	$x = 0.5$ textured	$x = 1.0$ random	$x = 1.0$ textured
Relative density (%)	95.3	92.1	97.0	95.4	98.1	96.3
T_{o-t} (°C)	210	209	193	187	191	183
T_c (°C)	420	420	418	416	417	415
ϵ_r	296	285	211	213	198	202
$\tan \delta$	0.028	0.044	0.011	0.014	0.007	0.016
d_{33} (pC/N)	110	135	91	137	85	146
k_p	0.33	0.45	0.31	0.54	0.31	0.58
k_{31}	0.20	0.29	0.18	0.32	0.17	0.33
Q_m	89	144	435	299	627	382

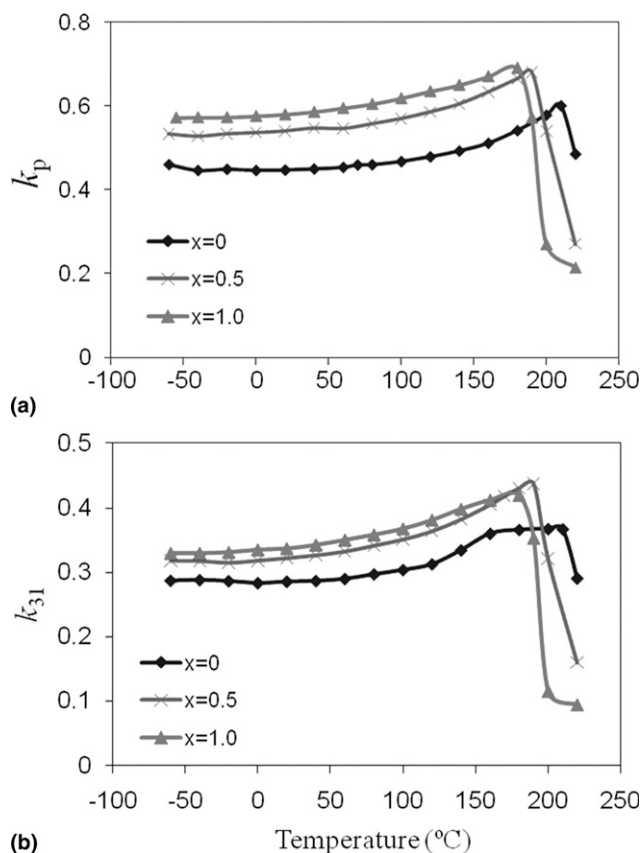


FIG. 9. Temperature dependence of electromechanical-coupling factors (a) k_p and (b) k_{31} for textured KNN- x mol% CuO ceramics sintered at 1150 °C for 8 h, 1135 °C for 3 h, and 1125 °C for 3 h, respectively.

CuO, as also can be seen for randomly oriented ceramics in Table I. In KNN materials, Cu^{2+} is incorporated into the perovskite B-site as an acceptor dopant, replacing Nb^{5+} . The lower charge of Cu^{2+} is compensated by oxygen vacancies, which clamp domain wall movement and lead to a lower piezoelectric constant d_{ijk} and a higher mechanical quality factor Q_m . However, in the case of textured KNN ceramics, the addition of CuO strongly promotes densification and grain growth, resulting in greatly improved density and texture quality compared with pure KNN. The resulting improvement in the piezo-

electric response due to texture quality outweighs the concurrent reduction in response caused by CuO acceptor doping. In contrast to d_{33} , the k_p and k_{31} for randomly oriented ceramics in Table I are only slightly reduced by the addition of CuO (and are also less dependent on the PPT temperature). Thus, the coupling coefficients are more useful for comparing these results to those of other studies on textured piezoelectric ceramics. The k_p value obtained from the textured ceramics with $x = 1.0$ in this work is high compared with other reports on CuO-doped KNN^{13–16} and is higher than that of most modified KNN ceramics with a PPT near room temperature.^{6–11}

Figure 9(a) shows the temperature dependence of k_p for textured KNN- x mol% CuO ceramics. The k_p values increase gradually on heating from -50 °C to the PPT temperature, after which they drop sharply. Textured KNN-1 mol% CuO has a k_p above 0.57 over the entire -50 to 180 °C temperature range. The k_{31} values [shown in Fig. 9(b)] of textured KNN show nearly identical temperature trends. The results confirm that CuO-doped textured KNN exhibits stable piezoelectric performance over a wide temperature range from $(-50$ °C to ~ 180 °C) compared with other KNN-based systems.

IV. CONCLUSIONS

Highly textured KNN was prepared by TGG using a two-step thermal process with CuO as a liquid phase sintering aid. Sintering at 1115 °C for 4 h in O_2 results in densification while preserving the NaNbO_3 template particles; sintering above this temperature destroyed the templates by reaction with the KNN matrix. While holding at this temperature for longer times resulted in some texture development, the highest degrees of texture were produced by using higher annealing temperatures (between 1125 and 1150 °C), depending on CuO concentration. In all cases, the templates begin to grow only once the ceramic reaches about 92% of the theoretical density. A Lotgering factor F_{001} of $\sim 99\%$ and a rocking curve FWHM of 6.9° were obtained by using 1 mol% CuO as the sintering aid. KNN-1 mol% CuO shows a uniform microstructure of highly aligned, well-faceted grains.

The high degree of $\langle 001 \rangle$ orientation and high density resulting from two-step thermal processing of 1% CuO-doped KNN result in highly enhanced piezoelectric properties ($k_p \approx 0.58$, $k_{31} \approx 0.33$, and $d_{33} \approx 146$ pC/N) without a significant reduction in the PPT temperature. The d_{33} , k_p , and k_{31} of textured KNN–1% CuO are approximately 70%, 90%, and 90% greater than those of randomly oriented samples, respectively, and this high performance is observed from -50 to 180 °C. Because of the very strong dependence of d_{33} on compositional factors such as acceptor doping and shifts in PPT temperature, the coupling coefficients k_p and k_{31} are more useful properties for comparing these materials with other textured KNN based ceramics.

REFERENCES

1. B. Jaffe, W.R. Cook, and H. Jaffe: *Piezoelectric Ceramics* (Academic, New York, 1971), p. 135.
2. T.R. Shrout and S.J. Zhang: Lead-free piezoelectric ceramics: Alternatives for PZT? *J. Electroceram.* **19**, 111 (2007).
3. A. Safari and E.K. Akdoğan: *Piezoelectric and Acoustic Materials for Transducer Applications* (Springer, New York, 2008), p. 81.
4. L. Egerton and D.M. Dillon: Piezoelectric and dielectric properties of ceramics in the system potassium–sodium niobate. *J. Am. Ceram. Soc.* **42**, 438 (1959).
5. Y. Saito, H. Takao, T. Tani, T. Nonoyama, K. Takatori, T. Homma, T. Nagaya, and M. Nakamura: Lead-free piezoceramics. *Nature* **432**, 84 (2004).
6. S.J. Zhang, R. Xia, T.R. Shrout, G.Z. Zang, and J.F. Wang: Piezoelectric properties in perovskite $0.948(\text{K}_{0.5}\text{Na}_{0.5})\text{NbO}_3$ – 0.052LiSbO_3 lead-free ceramics. *J. Appl. Phys.* **100**, 104108 (2006).
7. Y.F. Chang, Z.P. Yang, Y.T. Hou, Z.H. Liu, and Z.L. Wang: Effect of Li content on the phase structure and electrical properties of lead-free $(\text{K}_{0.46-x/2}\text{Na}_{0.54-x/2}\text{Li}_x)(\text{Nb}_{0.76}\text{Ta}_{0.20}\text{Sb}_{0.04})\text{O}_3$ ceramics. *Appl. Phys. Lett.* **90**, 232905 (2007).
8. Y. Dai, X. Zhang, and G. Zhou: Phase transitional behavior in $(\text{K}_{0.5}\text{Na}_{0.5})\text{NbO}_3$ – LiTaO_3 ceramics. *Appl. Phys. Lett.* **90**, 262903 (2007).
9. E.K. Akdoğan, K. Kerman, M. Abazari, and A. Safari: Origin of high piezoelectric activity in ferroelectric $(\text{K}_{0.44}\text{Na}_{0.52}\text{Li}_{0.04})(\text{Nb}_{0.84}\text{Ta}_{0.10}\text{Sb}_{0.06})\text{O}_3$ ceramics. *Appl. Phys. Lett.* **92**, 112908 (2008).
10. K. Wang, J.F. Li, and N. Liu: Piezoelectric properties of low-temperature sintered Li-modified $(\text{Na}, \text{K})\text{NbO}_3$ lead-free ceramics. *Appl. Phys. Lett.* **93**, 092904 (2008).
11. Y.F. Chang, Z.P. Yang, D.F. Ma, Z.H. Liu, and Z.L. Wang: Phase transitional behavior, microstructure, and electrical properties in Ta-modified $[(\text{K}_{0.458}\text{Na}_{0.542})_{0.96}\text{Li}_{0.04}]\text{NbO}_3$ lead-free piezoelectric ceramics. *J. Appl. Phys.* **104**, 024109 (2008).
12. R. Zuo, J. Rodel, R. Chen, and L. Li: Sintering and electrical properties of lead-free $\text{Na}_{0.5}\text{K}_{0.5}\text{NbO}_3$ piezoelectric ceramics. *J. Am. Ceram. Soc.* **89**, 2010 (2006).
13. D.M. Lin, K.W. Kwok, and H.L.W. Chan: Double hysteresis loop in Cu-doped $\text{K}_{0.5}\text{Na}_{0.5}\text{NbO}_3$ lead-free piezoelectric ceramics. *Appl. Phys. Lett.* **90**, 232903 (2007).
14. H. Park, J. Choi, M. Choi, K. Cho, S. Nahm, H. Lee, and H. Kang: Effect of CuO on the sintering temperature and piezoelectric properties of $(\text{Na}_{0.5}\text{K}_{0.5})\text{NbO}_3$ lead-free piezoelectric ceramics. *J. Am. Ceram. Soc.* **91**, 2374 (2008).
15. M. Matsubara, T. Yamaguchi, W. Sakamoto, K. Kikuta, T. Yogo, and S. Hirano: Processing and piezoelectric properties of lead-free $(\text{K}, \text{Na})(\text{Nb}, \text{Ta})\text{O}_3$ ceramics. *J. Am. Ceram. Soc.* **88**, 1190 (2005).
16. S.J. Zhang, J.B. Lim, H.J. Lee, and T.R. Shrout: Characterization of hard piezoelectric lead-free ceramics. *IEEE Trans. Ultrason. Ferroelectr. Freq. Control* **56**, 1523 (2009).
17. K.H. Brosnan, S.F. Poterala, R.J. Meyer, S. Misture, and G.L. Messing: Templated grain growth of $\langle 001 \rangle$ textured PMN–28PT using SrTiO_3 templates. *J. Am. Ceram. Soc.* **92**, s133 (2009).
18. H. Amorín, I. Santacruz, J. Holc, M.P. Thi, M. Kosec, R. Moreno, and M. Algueró: Tape-casting performance of ethanol slurries for the processing of textured PMN–PT ceramics from nanocrystalline powder. *J. Am. Ceram. Soc.* **92**, 996 (2009).
19. T. Richter, S. Dennerler, C. Schuh, E. Suvaci, and R. Moos: Textured PMN–PT and PMN–PZT. *J. Am. Ceram. Soc.* **91**, 929 (2008).
20. T. Shoji, K. Fuse, and T. Kimura: Mechanism of texture development in $\text{Bi}_{0.5}(\text{Na}, \text{K})_{0.5}\text{TiO}_3$ prepared by the templated grain growth process. *J. Am. Ceram. Soc.* **92**, S140 (2009).
21. K. Fuse, and T. Kimura: Effect of particle sizes of starting materials on microstructure development in textured $\text{Bi}_{0.5}(\text{Na}_{0.5}\text{K}_{0.5})_{0.5}\text{TiO}_3$. *J. Am. Ceram. Soc.* **89**, 1957 (2006).
22. C. Duran, S. Trolier-Mckinstry, and G.L. Messing: Dielectric and piezoelectric properties of textured $\text{Sr}_{0.53}\text{Ba}_{0.47}\text{Nb}_2\text{O}_6$ ceramics prepared by templated grain growth. *J. Mater. Res.* **18**, 228 (2003).
23. G.L. Messing, S. Trolier-McKinstry, E.M. Sabolsky, C. Duran, S. Kwon, B. Brahmaroutu, P. Park, H. Yilmaz, P.W. Rehrig, K.B. Eitel, E. Suvaci, M. Seabaugh, and K.S. Oh: Templated grain growth of textured piezoelectric ceramics. *Crit. Rev. Solid State Mater. Sci.* **29**, 45 (2004).
24. H. Takao, Y. Saito, Y. Aoki, and K. Horibuchi: Microstructural evolution of crystalline-oriented $(\text{K}_{0.5}\text{Na}_{0.5})\text{NbO}_3$ piezoelectric ceramics with a sintering aid of CuO. *J. Am. Ceram. Soc.* **89**, 1951 (2006).
25. Y.F. Chang, S. Poterala, Z.P. Yang, S. Trolier-McKinstry, and G.L. Messing: $\langle 001 \rangle$ textured $(\text{K}_{0.5}\text{Na}_{0.5})(\text{Nb}_{0.97}\text{Sb}_{0.03})\text{O}_3$ piezoelectric ceramics with high electromechanical coupling over a broad temperature range. *Appl. Phys. Lett.* **95**, 232905 (2009).
26. Y.F. Chang, Z.P. Yang, X.L. Chao, Z.H. Liu, and Z.L. Wang: Synthesis and morphology of anisotropic NaNbO_3 seed crystals. *Mater. Chem. Phys.* **111**, 195 (2008).
27. F.K. Lotgering: Topotactical reactions with ferrimagnetic oxides having hexagonal crystal structures. *J. Inorg. Nucl. Chem.* **9**, 113 (1959).
28. *IEEE Standard on Piezoelectricity* (American National Standards Institute, New York, 1987).
29. S.J. Zhang, E.F. Alberta, R.E. Eitel, C.A. Randall, and T.R. Shrout: Elastic, piezoelectric, and dielectric characterization of modified BiScO_3 – PbTiO_3 ceramics. *IEEE Trans. Ultrason. Ferroelectr. Freq. Control* **52**, 2131 (2005).
30. V.P. Sirovinkin and N.M. Drozdova: Interaction in binary system of CuO – Nb_2O_5 . *Russ. J. Inorg. Chem.* **37**, 1334 (1992).